Agricultural Water Management 266 (2022) 107516

Contents lists available at ScienceDirect

Agricultural Water Management

journal homepage: www.elsevier.com/locate/agwat

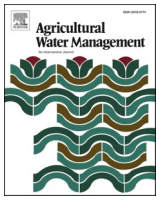

UAV-based multispectral vegetation indices for assessing the interactive effects of water and nitrogen in irrigated horticultural crops production under tropical sub-humid conditions: A case of African eggplant

Paul Reuben Mwinuka [a,*], Sixbert K. Mourice [b], Winfred B. Mbungu [a], Boniphace P. Mbilinyi [a], Siza D. Tumbo [c], Petra Schmitter [d]

[a] Sokoine University of Agriculture, Department of Civil and Water Resources Engineering, Tanzania
[b] Sokoine University of Agriculture, Department of Crop Science and Horticulture, Tanzania
[c] Ministry of Agriculture, Tanzania
[d] International Water Management Institute (IWMI), Sri Lanka

ARTICLE INFO

Handling Editor - J.E. Fernández

Keywords:
Water use efficiency
Nitrogen use efficiency
UAV
Irrigation
Water stress
Vegetation indices

ABSTRACT

UAV-based multispectral vegetation indices are often used to assess crop performance and water consumptive use. However, their ability to assess the interaction between water, especially deficit irrigation, and nitrogen application rates in irrigated agriculture has been less explored. Understanding the effect of water-nitrogen interactions on vegetation indices could further support optimal water and N management. Therefore, this study used a split plot design with water being the main factor and N being the sub-factor. African eggplants were drip irrigated at 100% (I100), 80% (I80) or 60% (I60) of the crop water requirements and received 100% (F100), 75% (F75), 50% (F50) or 0% (F0) of the crop N requirements. Results showed that the transformed difference vegetation index (TDVI) was best in distinguishing differences in leaf moisture content (LMC) during the vegetative stage irrespective of the N treatment. The green normalized difference vegetation index (GNDVI) worked well to distinguish leaf N during vegetative and full vegetative stages. However, the detection of the interactive effect of water and N on crop performance required a combination of GNDVI, NDVI and OSAVI across both stages as each of these 3 VI showed an ability to detect some but not all treatments. The fact that a certain amount of irrigation water can optimize the efficiency of N uptake by the plant is an important criterion to consider in developing crop specific VI based decision trees for crop performance assessments and yield prediction.

1. Introduction

Assessing the interactive effect of water and nitrogen for agriculture has been on top of the world agenda. This is because, there is a large gap between currently observed crop yields and the attainable yields when water and nitrogen are supplied in adequate amounts in different areas, especially in less developed countries (Qin, 2015). Water and nitrogen (N) deficiency are frequently limiting factors for crop production and they often occur together (Klem et al., 2018). To minimize risk of yield reductions due to N limitations, farmers often apply excessive fertilizer. However, the translation of N application into vegetable crop production is strongly dependent on adequate and timely water management (Zotarelli et al., 2009). Hence, effective, and efficient translation of water and nitrogen into agricultural productions requires studies to look at the interactive effects of water and nitrogen influencing plant growth and therefore biomass accumulation. Higher level of biomass accumulation has been linked with an increase in crop yield (Cambui et al., 2011; Chen et al., 2018). This is more evident in horticultural crops production where higher seasonal yields are associated with the level of biomass accumulation (Liu et al., 2014; Moncada et al., 2020).

Most farmers in Sub-saharan Africa use traditional practices to manage water and nitrogen (El Nahry et al., 2011). Traditional methods of decision making use visual observation of plant canopy responses to manage water and nitrogen inputs. Studies have shown that visual signs of nutrient deficiency occur while the plant is already experiencing significant levels of stress (Mee et al., 2017; Park et al., 2015). At that

* Corresponding author.
E-mail addresses: reubenpal@sua.ac.tz, reubenpal@gmail.com (P.R. Mwinuka).

https://doi.org/10.1016/j.agwat.2022.107516
Received 15 December 2020; Received in revised form 18 January 2022; Accepted 28 January 2022
Available online 17 March 2022

point often yield reductions will already be inevitable. Furthermore, the methods are not capable of estimating the amount of inputs to apply, resulting into under or over application of water and/or nitrogen (Tripathi et al., 2017). Over irrigation on its turn results into low fertilizer use efficiency, reduced productivity, and increased production costs (Yuan and Peng, 2017). Higher water application may also result into nitrogen leaching leading to pollution of water bodies and wider environmental pollution.

To improve water and N use efficiencies it requires effective management of both resources in tandem. Several methods to determine water stress have been used in irrigation scheduling over years. The methods have been categorized into soil-based and plant based techniques (Mwinuka et al., 2021b). Some of the soil based methods are soil moisture monitoring using soil moisture sensors such as time domain reflectometry (TDR), tension meters and neutron probes (Benor et al., 2013; Restuccia, 2021). However, the use of soil moisture sensors provides point based soil moisture values and might fail to capture field heterogeneity resulting in spatial variation of plant water stress and therefore crop performance (Mwinuka et al., 2021b). On the other hand, plant canopy-based methods have been used in crop water status monitoring as signs of canopy stress occur earlier than soil-based signs (Poblete-Echeverría et al., 2017; Petrie et al., 2019). These methods are characterized into contact and non-contact. Examples of contact methods are leaf diffusion porometers and pressure chamber for measuring stomatal conductance and water potential (Berni et al., 2009; Poblete-Echeverría et al., 2017). Non-contact methods include infrared thermometers, mobile phone-based thermal imaging and remote sensing among others (Çolak et al., 2015; Stone et al., 2016; Petrie et al., 2019).

Field nitrogen assessment has predominantly focused on plant canopy based indicators due to the complexity of measuring soil parameters even with the latest advances in rapid in-situ soil diagnostics. Plant canopy nitrogen management has been possible due to physiological and biochemical changes occurring within the plant under certain conditions (Fang et al., 2017; Klem et al., 2018). These changes within the plant canopy result into differences in solar radiation reflectance of the electromagnetic spectrum. The analysis of these differences in reflectance results into identification of the level of N composition within the plant canopy and hence enhances management decisions. Canopy reflectance and derived plant N status can be captured by portable spectroradiometers, hand-held plant chlorophyll meters and remote sensing techniques (Julitta et al., 2016; Irfan et al., 2018).

So far, mainly canopy based methods are used to look at the interactive effect of water and nitrogen, these include isotopic techniques as well as low altitude remote sensing methods (Bronson et al., 2017; Klem et al., 2018). Low altitude remote sensing techniques have been effectively conducted using multispectral and hyperspectral sensors, with the earlier being more affordable and capable in collecting detailed plant information (Badzmierowski et al., 2019; Bhandari et al., 2018). This technology uses different spectral bands such as visible spectral (red, green and blue), near infrared (IR) and short-wave infrared ranges. Multispectral range contains 3–10 bands while hyperspectral comprise hundreds of narrow bands (Corti et al., 2017). Within the multispectral region, high reflectance from the leaf mesophyll in healthy plant canopy falls within the near infrared region (Reyes-Gonzalez, 2017).

Several vegetation indices have been used to assess water and nitrogen in different crops such as wheat, corn, tomatoes, lettuce and spinach under different climatic conditions (Bronson et al., 2017; Cabrera-Bosquet et al., 2011; Elvanidi et al., 2018; Ge et al., 2019; Klem et al., 2018; Shiratsuchi et al., 2011; Bhandari et al., 2018). Most of these studies have shown variation of various vegetation indices in assessing water and N separately. Few studies have assessed the ability of the vegetation indices in assessing the interactive effects of water and N despite the fact that deficiencies frequently occur together (Klem et al., 2018). Likewise, spectral behavior of crops differs with climatic conditions and crop type (Bellvert et al., 2015).

Studies of spectral responses of horticultural crops to different combinations of water and nitrogen stress in tropical sub-humid regions are less studied. Therefore, this study aimed to assess the efficacy of vegetation indices in evaluating different levels of crop water and N management. This study is aimed at enhancing service delivery by public or private sector extension services for small, medium and large-scale farming to enhance yields, and water use and N use efficiencies (Mwinuka et al., 2021b). The study investigated the use of UAV-derived multispectral vegetation indices in assessing the effect of different water and nitrogen management strategies in horticultural crops. The specific objectives were to: (1) assess the variation of vegetation indices to nitrogen treatments at different irrigation depths (2) investigate vegetation indices response to water, N and their interaction (3) assess the effectiveness of vegetation indices maps to distinguish different water and N strategies, and (4) assess the relationship of potential vegetation indices with fruit yield as a result of water and N management.

2. Materials and methods

2.1. Experimental site

The study was conducted at Rudewa ward, Kilosa district in Morogoro region, Tanzania (Fig. 1). The ward is between 6°32' to 6°47' South and 36°8' to 37°28' East. The average altitude of the study site is 437 m above mean sea level and average annual temperature ranges between 15.1 °C and 24.4 °C. The minimum temperature is recorded in July while the maximum temperature of 32.1 °C is recorded in February. The mean relative humidity is 67.5%. The area has a bimodal rainfall regime with short rains occurring from October to December while long rains from March to May. The annual average rainfall ranges between 1000 mm and 1400 mm.

Irrigated agriculture is commonly practiced during the dry period June to November and the short rainy period December to February. The major source of irrigation water is the Wami River which flows from the Mamiwa Forest Reserve throughout the year. Soils are predominantly sand clayey loamy soils with a medium level of organic carbon. The clay, silt and sand content range between 23% and 26%, 10% − 14% and 58–65% respectively within the top 40 cm. The average soils bulk density within the study sites was 1.3 – 1.5 g/cm^3.

2.2. Experimental design

The experiment was laid out in a 3 × 4 arrangement of treatments under a split plot design (Fig. 2) with irrigation water being the main plot and N the subplot (Kadiyala, 2012). There were 3 irrigation treatments each with 4 levels of N application. Irrigation water treatments were 100% (I100), 80% (I80) and 60% (I60) of crop water requirements for eggplant under drip irrigation. N fertilizer treatments were 100% (F100), 75% (F75), 50% (F50) and 0% (F0) of crop N requirements, respectively. Each treatment was repeated three times.

The plot size for each replicate was 35 m^2 with plant and row spacing of 60 cm and 90 cm respectively. Transplanting was conducted on the top of the ridges where driplines were installed. The experiment was conducted during the dry seasons June to October 2017 and 2018.

2.3. Irrigation water requirements and nitrogen application

Crop water requirements were estimated using CROPWAT 8.0 software as recommended by FAO using 15 years of climatic data from Ilonga meteorological station (Mwinuka et al., 2021a). The crop coefficient (Kc) and the reference evapotranspiration (ETo) were used to estimate the crop actual evapotranspiration (ETc) (Table 1). The ETc was used to calculate the daily net irrigation water requirements (IWRn) and ultimately the gross irrigation requirements (GIWR) as shown in Table 1.

Microclimate data from an automatic weather station installed 500 m away from the field site were used to adjust daily irrigation water

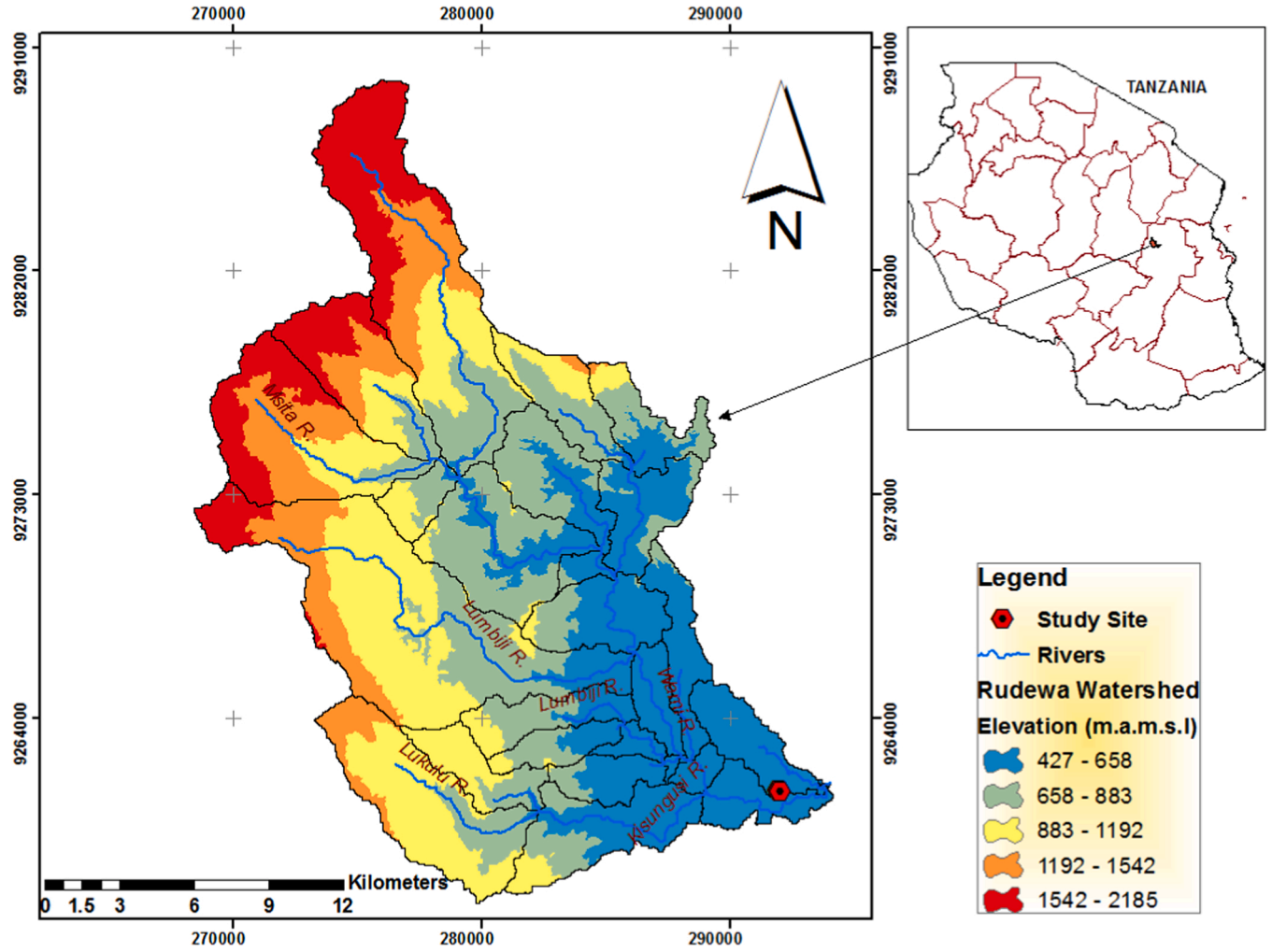

Fig. 1. The map showing the Rudewa ward study site within Kilosa district (Source: Mwinuka et al., 2021a).

requirement (Fig. 3). The crop evapotranspiration (ETc) at any time was adjusted using the crop coefficient (Kc) and crop reference evapotranspiration (ETo) using data recorded by an automatic weather station. The effective rainfall was estimated using USDA-SCS method as described by Patwardhan et al. (1990). The water requirement was further adjusted using the soil water balance method and moisture data from the DSMM500 moisture meter. The amount of irrigation water to be applied in each irrigation cycle was finally reduced depending on the treatment (i.e. 100%, 80% or 60% of the crop water requirement). The total amount of water applied throughout the season was 1035 mm, 828 mm and 621 mm for I100, I80 and I60, respectively.

Nitrogen was applied through Urea (46−0−0) at 7, 30, 60 and 90 days after transplanting, distributed as 16%, 34%, 34% and 16% of N respectively. The seasonal N applied was 250 kg/ha, 187 kg/ha, 125 kg/ha and 0 kg/ha for F100, F75, F50 and F0, respectively. Fertilizer recommendations for F100 were based on other crops within the solanaceae family such as eggplant and tomatoes (RSA, 2012; Fondio et al., 2016) grown under different climatic conditions in absence of local fertilizer recommendations.

2.4. Assessment of vegetation indices response to water, N and their interaction

2.4.1. Leaf nitrogen and water content assessment

Plant leaves from each plot were collected 3 times during early, vegetative and full vegetative stages. Leaf N content was determined using the Kjeldahl procedure on the third youngest fully developed leaf (Omer et al., 2017). The plant leaf water content was measured destructively by oven drying of the leaf samples at 70 °C until constant weight was attained (Ge et al., 2016). Leaves were harvested between 08:00 – 10:00 h, to minimize solar radiation errors through evaporation. Soon after harvesting, fresh leaves were weighted using class B digital weighing balance complying with Canadian ices-003. The leaf water content (LWC) was estimated using the fresh (Wl) and dry (Dl) sample weights as shown in Eq. (1).

$$LWC = \frac{Wl - Dl}{Wl} \times 100\% \quad (1)$$

2.4.2. UAV based images acquisition and processing

Images were acquired using a multispec4c sensor attached to the fixed wing UAV eBeeTM drone (a senseFly SA, Cheseaux-Lausanne, Switzerland) (Mwinuka et al., 2021b). The multispec4c sensor had green, red, red edge and near-infrared spectral bands with wavelengths of 550 nm, 660 nm, 735 nm and 790 nm respectively. The sensor had a ground sampling distance (GSD) of 12 cm/pixel and was set at a lateral and longitudinal overlap of 70% and 65%. The images were acquired within two hours (between 12:00–13:30) to minimize shadow effects using a UAV flown at an average altitude of 115 m above elevation data (AED). Production of orthomosaic maps from multispectral images was conducted using the PIX4D software (Pix4D SA, Lausanne, Switzerland).

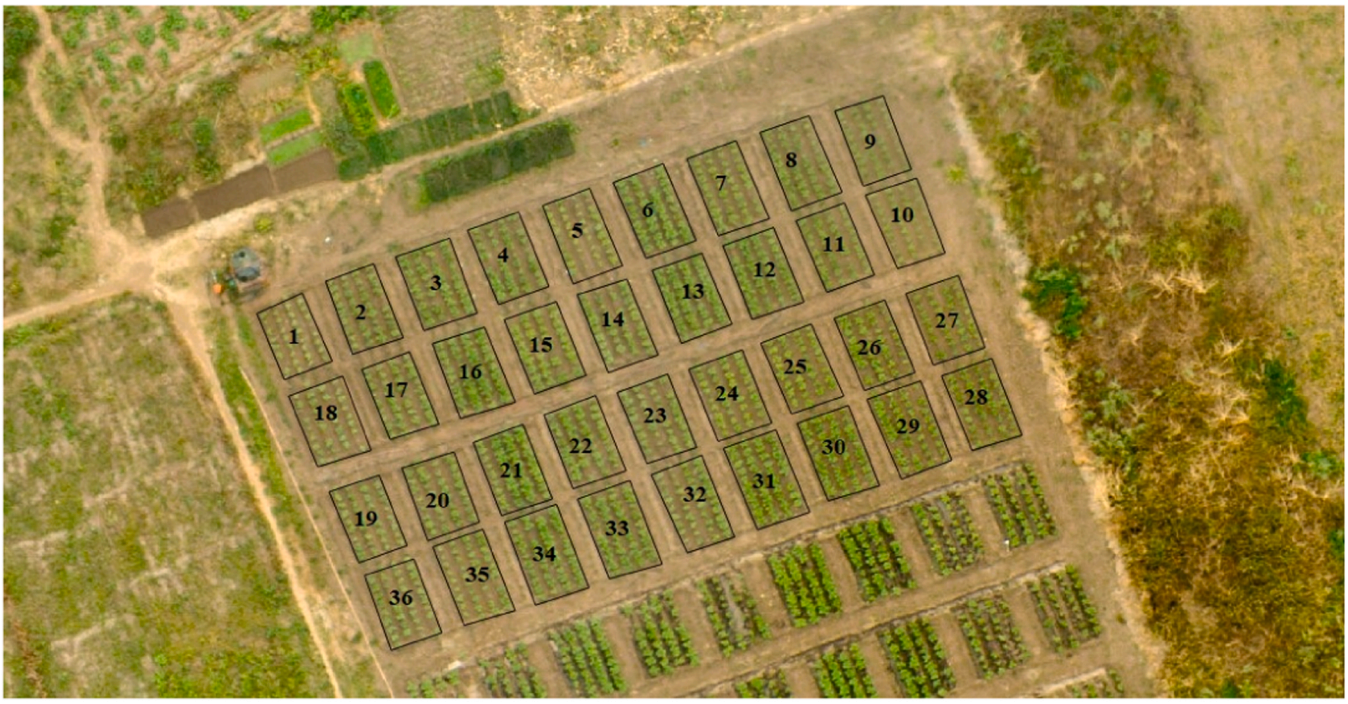

Fig. 2. Layout of the experimental field and respective sub-plot treatments. Note: Plots 12, 13 and 34 represent I100F100; 6,8 and 33 represent I100F75; 11,14 and 22 represent I100F50; 5,7 and 21 represent I100F0; 3, 23 and 30 represent I80F100; 4,29 and 32 represent I80F75; 16,26 and 31 represent I80F50; 15, 24 and 25 represent I100F0; 9, 17 and 19 represent I60F100; 2,28,36 represent I60F75; 18,20 and 27 represent I60F50; 1,10 and 35 represent I60F0.

Table 1
Crop evapotranspiration and irrigation water requirements at different cropping stages.

Month	Stage	Kc	ETo	ETc	Effective rainfall	IWRn	GIWR
		coefficient	mm/day	mm/day	mm	mm/day	mm/day
June	Early	0.6	3.4	2	0	2	2.4
July	Vegetative	0.7	3.4	2.4	0	2.4	2.8
July	Full vegetative	1.1	3.4	3.7	0.1	3.6	4.2
August	Full vegetative and late-season	1.1	3.7	4.1	0	4.1	4.8
September	Late-season	1.1	4.3	4.7	0	4.7	5.5
October	Late-season	1	4.9	4.9	0.2	4.7	5.5

Source: Mwinuka et al. (2021b).

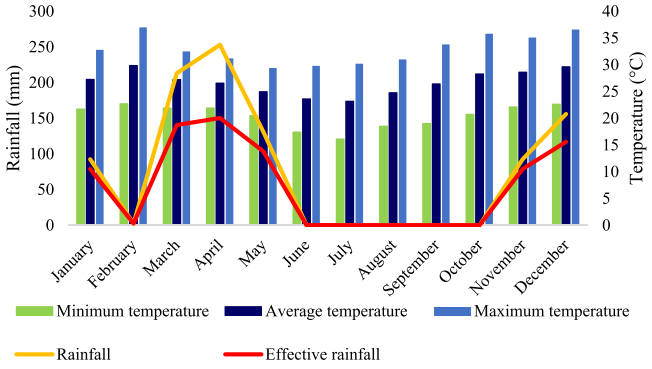

Fig. 3. Average microclimatic data for years 2017 and 2018 of the study site.

The details of the methodology is described by Mwinuka et al. (2021b).

The choice of vegetation indices (VI) was based on their capability to estimate leaf water content, leaf N and their interaction as reported by different scholars. The indices were limited to four spectral bands (green, red, near-infrared and red edge) within multispec4c sensor. Considering these 2 factors, the following indices were explored (Table 2):

Table 2
Vegetation indices of choice for assessing water and nitrogen.

S/N	Index	Reference
1	$GRVI = \frac{G-R}{G+R}$	Xue and Su (2017)
2	$NDVI = \frac{NIR-R}{NIR+R}$	Ustuner et al. (2014)
3	$GNDVI = \frac{NIR-G}{NIR+G}$	Omer et al. (2017)
4	$NDRE = \frac{NIR-RE}{NIR+RE}$	Ustuner et al. (2014)
5	$EVI2 = 2.5(\frac{NIR-R}{NIR+2.4R+1})$	Picoli et al. (2017)
6	$SAVI = \frac{1.5(NIR-R)}{NIR+R+0.5}$	Mulla (2013)
7	$OSAVI = \frac{(NIR-R)}{NIR+R+0.16}$	Zou and Mõttus (2017)
8	$TDVI = \sqrt{0.5+\frac{NIR-R}{NIR+R}}$	Xue and Su (2017)

0.16 for OSAVI = Soil adjustment coefficient to minimize the effect of soil background reflectance

2.4.3. Capability of vegetation indices to assess water, N and their interaction

The derived leaf water and N content were used to assess the suitability of the VIs in assessing water and N and their interaction at different crop stages. The analysis of variance (ANOVA) was used to assess whether the VIs differed significantly in function of the water and nitrogen treatment. The capability of VI to distinguish leaf water, N contents and the interactive effect of water and N was performed using the least significant difference (LSD) test at $p < 0.05$ and radar charts.

2.5. Effectiveness of vegetation indices maps to distinguish different water and N combinations

Vegetation indices maps were developed to spatially differentiate areas with different water and N combinations in the field (Mwinuka et al., 2021b). The image mosaic was processed in Rstudio software (version 3.6.1) handled in respective bands using raster and rgdal packages (Team, 2018). The plot function was further applied to generate vegetation indices maps.

2.6. The relationship between vegetation indices and fruit yield

The correlation between vegetation indices and fruit yield was assessed using the regression model. The software used was ggplot2 package under Rstudio version 3.6.1. The software was used to evaluate a linear relationship of fruit yield against the vegetation indices. Only results were considered where the coefficient of correlation (R^2) was at least 0.5.

3. Results

3.1. Variation of vegetation indices to nitrogen treatments at different irrigation depths

Vegetation indices have shown to respond differently to N at different cropping stages. The indices GNDVI, NDVI and OSAVI responded best to different N application rates at different irrigation treatments. Due to soil background reflectance, the early crop development stage had no significant difference found among N treatments for any of the irrigation treatments. At 100% (I100) irrigation depth, the GNDVI increased significantly with increased N application at vegetative and full vegetative stages (Fig. 4). In the vegetative and full vegetative stages for I80, two groups could be distinguished: F100 and F75 vs. F50 and F0 (Fig. 5). However, between F100 and F75 as well as between F50 and F0 no significant differences were found. Within the I60 treatment, the calculated VIs differed in function of N application between F100, F75 and F50 but not between F50 and F0 (Fig. 6).

Similarly, NDVI and OSAVI increased significantly when more N was applied at vegetative and full vegetative stages (Figure not shown). During the vegetative stage, the NDVI at I100 did not differ significantly between F100 and F75 (Figure not shown). Similar trends were observed for I80 and I60 irrigation treatments (Figure not shown). In all irrigation treatments, the NDVI for F0 was significantly lower compared to the rest. The OSAVI also showed a good response to N application at all irrigation regimes (Figure not shown). This is due to significant differences in the reflectance from the crop canopy as a result of water and nitrogen variation within the plant. Other vegetation indices such as GRVI, NDRE, EVI2, SAVI and TDVI also increased when higher amounts of N were applied under different irrigation regimes (Figure not shown). However, these indices were unable to differentiate between specific N-treatments.

3.2. The response of vegetation indices to the interactive effect of water and N

3.2.1. The response of vegetation indices to leaf moisture content at different irrigation levels

Vegetation indices had different responses to varying leaf moisture content (Table 3). At the vegetative stage, the TDVI had best performance in distinguishing the levels of canopy water stress at all levels of water application (I100, I80 and I60). The GNDVI, NDVI and OSAVI were not capable of distinguishing between I100 and I80 while they distinguished I60. SAVI distinguished the plant canopy under I100 from other treatments during vegetative and full vegetative stages. The EVI2, GRVI and NDRE did not pick up on canopy differences caused by water stress in the vegetative stage.

At the full vegetative stage, the EVI2, GNDVI, GRVI, NDVI, OSAVI and SAVI were all able to distinguish the high water stressed canopies under I60 from the other two treatments (Table 3). The TDVI and NDRE failed to differentiate treatments at full vegetative stage.

3.2.2. The response of vegetation indices to leaf N content at different N rates

The variation of leaf N content differed in function of the N applied resulting in differences in VI (Table 4). At the vegetative stage, GNDVI performed well in differentiating between F100, F75, F50 and F0. The GRVI, NDVI and OSAVI were capable of discriminating F0 from the rest of the treatments. SAVI, TDVI and NDRE had a weak capability to distinguish the plant N content irrespective of the irrigation treatment.

At the full vegetative stages, GNDVI performed best in differentiating between F100, F75, F50 and F0 (Table 4). The NDVI and OSAVI were capable of distinguishing F50 and F0 from the rest of the treatments. The rest of the vegetation indices (EVI2, GRVI, SAVI, TDVI and NDRE) had a weak performance in differentiating the variation of leaf N among

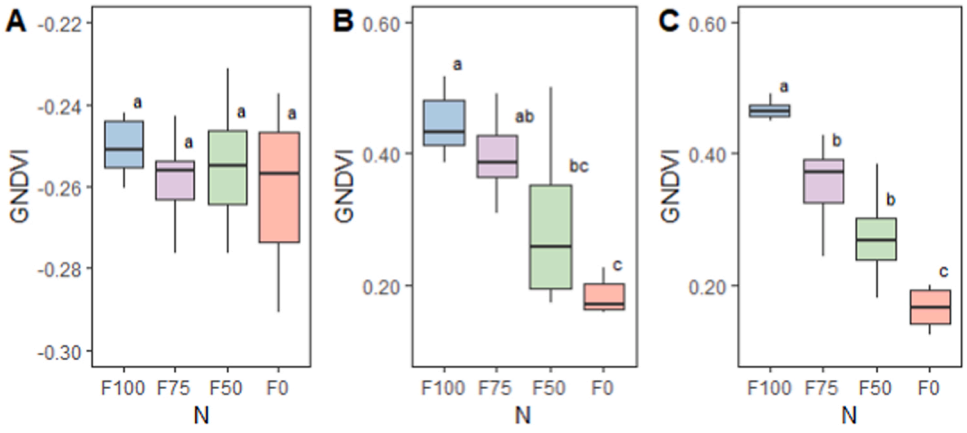

Fig. 4. GNDVI for treatments irrigated with 100% crop water requirements at early (A), vegetative (B) and full vegetative (C) stages of crop development.

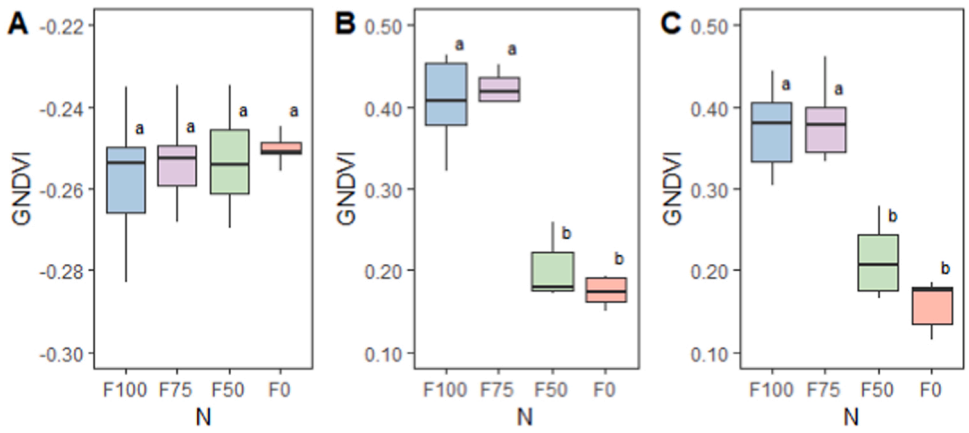

Fig. 5. GNDVI for treatments irrigated with 80% crop water requirements at early (A), vegetative (B) and full vegetative (C) stages of crop development.

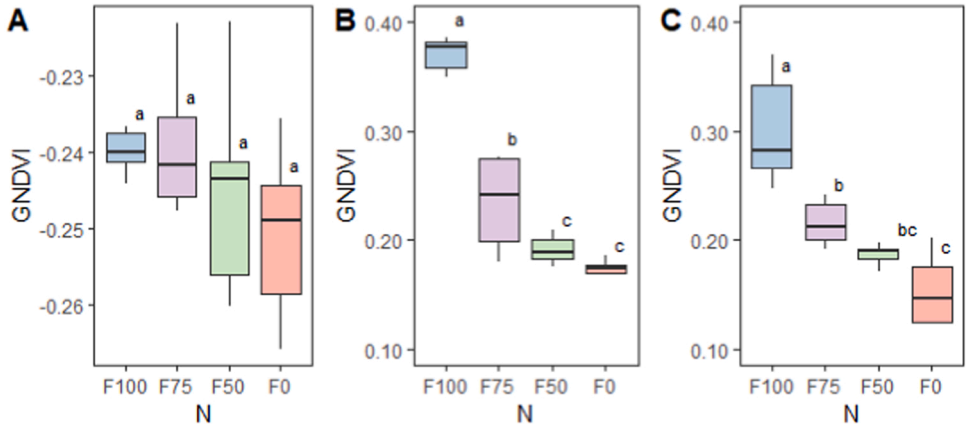

Fig. 6. GNDVI for treatments irrigated with 60% crop water requirements at early (A), vegetative (B) and full vegetative (C) stages of crop development.

Table 3
The average vegetation indices as a response to leaf moisture content at different irrigation levels.

WATER	EVI2	GNDVI	GRVI	NDVI	OSAVI	SAVI	TDVI	NDRE
Vegetative stage								
I100	0.4^{a}	0.3^{a}	0.3^{a}	0.56^{a}	0.55^{a}	0.4^{b}	0.7^{c}	-0.02^{a}
I80	0.5^{a}	0.3^{a}	0.3^{a}	0.58^{a}	0.57^{a}	0.5^{a}	0.72^{b}	0.01^{a}
I60	0.4^{a}	0.2^{b}	0.3^{a}	0.49^{b}	0.45^{b}	0.5^{a}	0.75^{a}	0.01^{a}
Full vegetative								
I100	0.5^{a}	0.3^{a}	0.3^{a}	0.49^{a}	0.47^{a}	0.4^{b}	0.8^{a}	-0.02^{a}
I80	0.4^{a}	0.3^{a}	0.34^{a}	0.46^{a}	0.44^{a}	0.5^{a}	0.8^{a}	0.01^{a}
I60	0.3^{b}	0.2^{b}	0.29^{b}	0.25^{b}	0.29^{b}	0.5^{a}	0.7^{a}	0.01^{a}

Numbers with the same letters are not statistically different at p = 0.05

Table 4
The average vegetation indices as a response to leaf N at different levels of N application.

N	EVI2	GNDVI	GRVI	NDVI	OSAVI	SAVI	TDVI	NDRE
Vegetative stage								
F100	0.5^{a}	0.4^{a}	0.32^{a}	0.57^{a}	0.54^{a}	0.5^{a}	0.7^{a}	-0.01^{a}
F75	0.5^{a}	0.3^{b}	0.32^{a}	0.56^{a}	0.53^{a}	0.5^{a}	0.7^{a}	0.01^{a}
F50	0.4^{a}	0.2^{c}	0.31^{ab}	0.53^{ab}	0.55^{a}	0.5^{a}	0.7^{a}	-0.01^{a}
F0	0.4^{b}	0.18^{d}	0.3^{b}	0.5^{b}	0.44^{b}	0.5^{a}	0.7^{a}	0.00^{a}
Full vegetative								
F100	0.5^{a}	0.4^{a}	0.34^{a}	0.5^{a}	0.48^{a}	0.5^{a}	0.8^{a}	-0.01^{a}
F75	0.4^{a}	0.36^{b}	0.34^{a}	0.46^{a}	0.46^{a}	0.5^{a}	0.7^{a}	0.01^{a}
F50	0.4^{a}	0.23^{c}	0.33^{a}	0.36^{b}	0.34^{b}	0.5^{a}	0.7^{a}	-0.01^{a}
F0	0.3^{a}	0.18^{d}	0.30^{a}	0.27^{c}	0.28^{c}	0.5^{a}	0.8^{a}	0.00^{a}

Numbers with the same letters are not statistically different at p = 0.05

treatments.

3.2.3. The response of vegetation indices to the interaction between water and N

Different vegetation indices performed differently in distinguishing the interactive effect of water and N (Table 4). The GNDVI, NDVI and OSAVI showed a stronger capability in distinguishing between the different water and N treatments at vegetative and full vegetative stages. The EVI2, GRVI, SAVI, TDVI and NDRE showed weak responses to the different treatments in all crop development stages (Table 5, Fig. 7).

During the vegetative stage, GNDVI showed the strongest capability in distinguishing between the various water and nitrogen treatments (Table 5 and Fig. 7). It was the only VI which was able to indicate a difference in canopy reflectance for I100F100 compared to the other treatments. Furthermore, GNDVI detected significant differences between the following 5 groups: 1) 100F100; 2) I100F75, I80F100 and I80F75; 3) I100F50 and I60F100; 4) I80F50 and I60F75; and 5) I100F0 and I60F0. Only I60F50 fell in both group 4 and group 5. NDVI performed reasonably well and was also able to detect 5 groups: 1) I100F100 and I100F75; 2) I80F100 and I80F75; 3) I80F50; 4) I80F0; 5) I100F0 and I60F0. However, NDVI was not able to detect differences among I60F100, I60F75, I60F50 and I100F75. OSAVI was also able to detect a few groups but overall performed less well compared to GNDVI and NDVI in the vegetative stage. OSAVI detected differences between groups: 1) I100F100 and I10075; 2) I100F50 and I80F50; 3) I60F0 but was unable to significantly detect differences in canopy reflectance for the other treatments.

At full vegetative stage, GNDVI performed less compared to the vegetative stage in detecting water and nitrogen treatment effects. GNDVI was able to only detect significant differences between I100F100, I100F50, I80F0 and I60F100. NDVI detected significant differences between 5 groups: 1) I100F100 and I100F75; 2) I60F75; 3) I100F50 and 4) I80F0 and I60F100 and 5) I60F0. However, these groups differed with those compared in the vegetative stage. OSAVI detected the same three groups as in the vegetative stage which were: 1) I100F100 and I100F75; 2) I100F50 and 3) I60F0.

3.3. Vegetation indices maps to assess the interactive effect of water and N

Based on the ability of the VI to detect differences in water and nutrient management, GNDVI and NDVI were used to develop the VI maps. The vegetation indices maps depicted well the spatial variability of water and N treatments in the field. At the full vegetative stage, GNDVI values ranged from − 0.29–0.52 with values between − 0.29–0.09 reflecting bare soils, and canopy reflectance under the various treatments between 0.1 and 0.52 (Fig. 8). The water and N combination which resulted in high yielding healthy plants showed a GNDVI in the range 0.35–5.2, moderate yielding plants between 0.25 and 0.35, and in stressed low yielding between 0.1 and 0.25.

Likewise, the NDVI showed spatial variability in function of the water and N treatment. Values during the full vegetative stage were in the range of − 0.3–0.76 (Fig. 8) with the canopy covered areas between 0.15 and 0.76. NDVI for the highest yielding treatments fell between 0.6 and 0.75, moderate yielding from 0.45 to 0.6 and low yielding treatments in the 0.1–0.3 range. The maps therefore, can be used to assess differences in canopy reflectance as a result of varying water and N conditions in the fields.

3.4. The correlation of the vegetation indices to the end of the season fruit yield

The correlation between the end of season yields and vegetation indices varied significantly. During the early development stage, there was a weak correlation of vegetation indices to the end of the season yields (Table 6). At the vegetative stage, the NDVI ($R^2 = 0.46$, $p = 4.7 \times 10^{-11}$) and OSAVI ($R^2 = 0.47$, $p = 4.1 \times 10^{-11}$) showed a moderate correlation with the end of season yields.

During the full vegetative stage, GNDVI showed a better correlation with the end of season yields ($R^2 = 0.47$, $p = 2.3 \times 10^{-11}$) compared to those in the vegetative stage (Table 6). The NDVI ($R^2 = 0.53$, $p = 5.9 \times 10^{-13}$) and OSAVI ($R^2 = 0.52$, $p = 2.8 \times 10^{-9}$) also showed a better correlation with the end of season yields at the full vegetative stage. However, the ability to use VI in yield predictions remains limited as they are able to predict around 50% of the obtained yields.

4. Discussion

4.1. The variation of vegetation indices to nitrogen treatments at different irrigation depths

Vegetation indices showed a varying capability to distinguish N at different irrigation depths. During the early cropping stages, none of the vegetation indices were capable of differentiating N at varying levels of irrigation. This is because most of the reflectance recorded was from the soil surface (Prudnikova et al., 2019). The GNDVI, NDVI and OSAVI could distinguish differences in canopy reflectance in function of N

Table 5
The average vegetation indices as a response to the interactive effect of water and N.

	Water x N treatment											
	I100F100	I100F75	I100F50	I100F0	I80F100	I80F75	I80F50	I80F0	I60F100	I60F75	I60F50	I60F0
Vegetative stage												
EVI2	0.48^{a}	0.46^{abc}	0.4^{bcde}	0.39^{cde}	0.47^{ab}	0.48^{a}	0.49^{a}	0.37^{de}	0.45^{abcd}	0.46^{abc}	0.43^{abcde}	0.35^{e}
GNDVI	0.43^{a}	0.35^{b}	0.27^{c}	0.16^{e}	0.37^{b}	0.38^{b}	0.21^{d}	0.16^{e}	0.3^{c}	0.22^{d}	0.18^{de}	0.15^{e}
GRVI	0.34^{ab}	0.33^{abc}	0.3^{cd}	0.31^{bcd}	0.33^{abc}	0.33^{abc}	0.35^{a}	0.31^{bcd}	0.31^{bcd}	0.32^{bc}	0.31^{cd}	0.28^{d}
NDVI	0.59^{a}	0.57^{a}	0.45^{de}	0.23^{g}	0.52^{b}	0.54^{b}	0.45^{c}	0.25^{f}	0.42^{cd}	0.41^{cde}	0.43^{cd}	0.2^{g}
OSAVI	0.58^{a}	0.57^{a}	0.47^{c}	0.22^{ef}	0.52^{b}	0.54^{ab}	0.46^{c}	0.23^{ef}	0.41^{cd}	0.43^{cd}	0.42^{cd}	0.20^{f}
SAVI	0.46^{abcd}	0.42^{bcd}	0.4^{d}	0.45^{abcd}	0.41^{cd}	0.47^{abcd}	0.54^{a}	0.5^{abcd}	0.48^{abcd}	0.51^{abc}	0.52^{ab}	0.48^{abcd}
TDVI	0.74^{abc}	0.66^{d}	0.7^{bcd}	0.72^{abcd}	0.68^{cd}	0.72^{abcd}	0.76^{ab}	0.74^{abc}	0.74^{abc}	0.78^{a}	0.76^{ab}	0.73^{abc}
NDRE	-0.02^{a}	-0.02^{a}	-0.03^{a}	-0.02^{a}	0.03^{a}	0.03^{a}	0.01^{a}	-0.01^{a}	-0.04^{a}	0.04^{a}	0.00^{a}	0.03^{a}
Full vegetative stage												
EVI2	0.53^{a}	0.53^{a}	0.40^{a}	0.35^{a}	0.47^{a}	0.45^{a}	0.47^{a}	0.38^{a}	0.36^{a}	0.3^{a}	0.31^{a}	0.28^{a}
GNDVI	0.46^{a}	0.4^{bc}	0.29^{d}	0.18^{ef}	0.41^{bc}	0.44^{ab}	0.21^{ef}	0.17^{f}	0.37^{c}	0.23^{de}	0.19^{ef}	0.18^{ef}
GRVI	0.37^{a}	0.37^{a}	0.33^{ab}	0.31^{ab}	0.33^{ab}	0.34^{ab}	0.36^{ab}	0.33^{ab}	0.31^{ab}	0.31^{ab}	0.3^{ab}	0.28^{b}
NDVI	0.63^{a}	0.62^{a}	0.43^{d}	0.29^{f}	0.58^{ab}	0.55^{abc}	0.40^{de}	0.29^{f}	0.28^{f}	0.23^{c}	0.26^{fg}	0.23^{g}
OSAVI	0.61^{a}	0.60^{a}	0.42^{d}	0.27^{de}	0.57^{ab}	0.52^{abc}	0.40^{cd}	0.31^{de}	0.26^{de}	0.26^{de}	0.25^{de}	0.21^{e}
SAVI	0.52^{ab}	0.33^{b}	0.38^{ab}	0.36^{ab}	0.49^{ab}	0.55^{ab}	0.40^{ab}	0.54^{ab}	0.40^{ab}	0.47^{ab}	0.61^{a}	0.54^{ab}
TDVI	0.81^{a}	0.71^{a}	0.77^{a}	0.77^{a}	0.79^{a}	0.76^{a}	0.72^{a}	0.77^{a}	0.70^{a}	0.73^{a}	0.72^{a}	0.76^{a}
NDRE	0.07^{a}	0.07^{a}	0.09^{a}	0.02^{a}	0.10^{a}	0.10^{a}	0.09^{a}	0.05^{a}	0.13^{a}	0.11^{a}	0.15^{a}	0.15^{a}

Note: Numbers with the same letter are not statistically different at p = 0.05

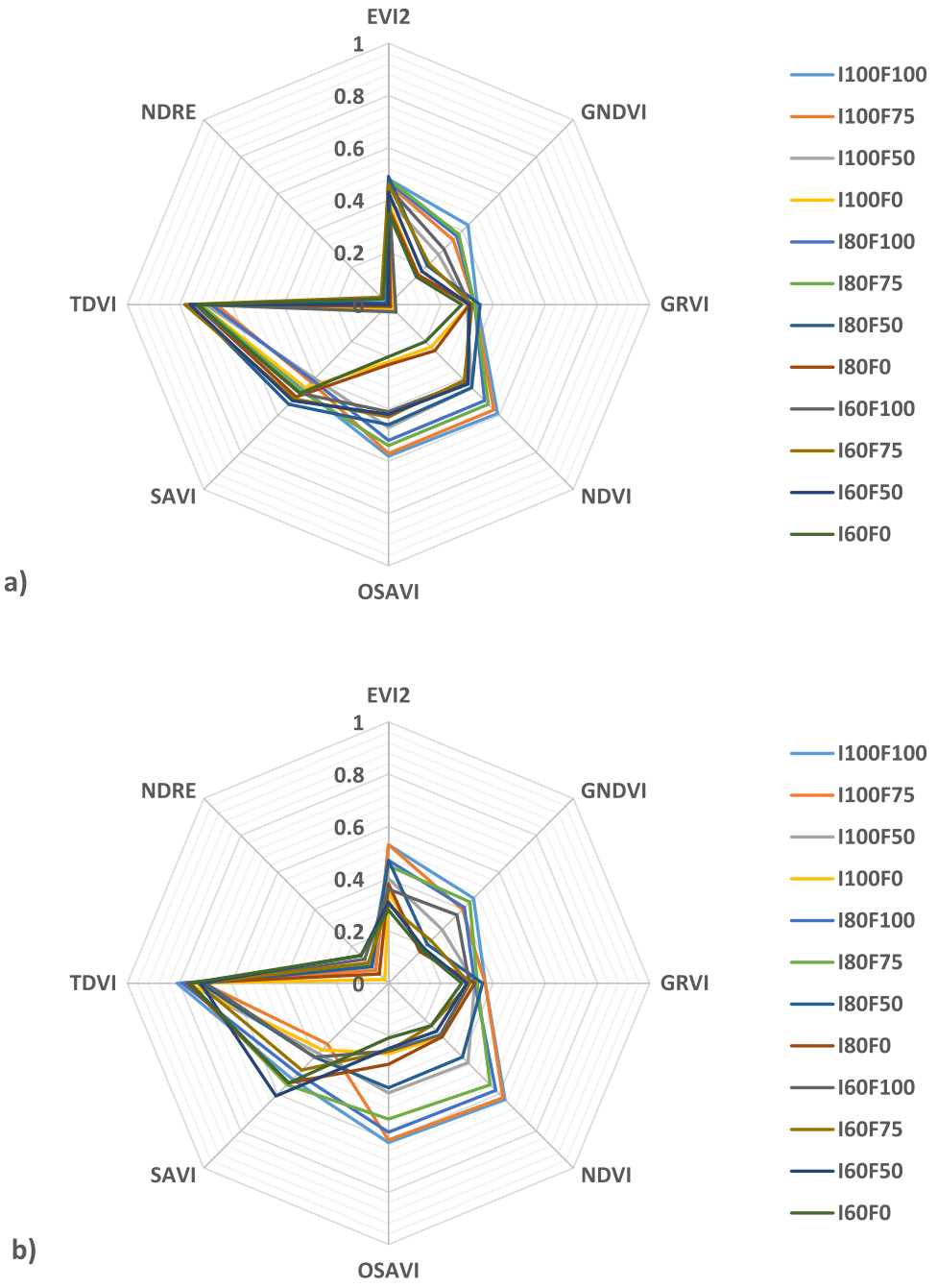

Fig. 7. Radar chart showing the average vegetation indices in function of the water and nitrogen treatment at a) the vegetative stage and b) the full vegetative stage.

application at vegetative and full vegetative stages across irrigation treatments. This is related to the response of these VIs to the chlorophyll and xanthophyll content which are related to crop water status (Zhang et al., 2019).

These findings are similar to earlier studies which assessed plant water status at varying N levels in different crops. Zhang et al. (2019) recommended the use of NDVI in irrigation water management of maize crops due to its response to water stress. Bhandari et al. (2018) got weak correlation of all NDVI and GNDVI on their response to water, N and their interaction in lettuce. Weak correlation of these vegetation indices in the lettuce crop might be caused by differences in chemical characteristics and leaf morphology of the canopy surface resulting in different responses to the incoming solar radiation. Shiratsuchi et al. (2011) selected the red edge NDVI and the red band NDVI as they were capable at distinguishing the crop performance variation due to different irrigation levels and showed average capability to distinguish between N rates in corn production.

Canopy N content was distinguished by different vegetation indices within the vegetative and full vegetative stages. The study observed the capability of GNDVI, NDVI and OSAVI in distinguishing leaf N at different water regimes during the vegetative and full vegetative stages. Furthermore, in the full vegetative, GNDVI performed slightly better than NDVI and OSAVI in its ability to detect differences in N application rates in the I100 and I60 treatments, less so in the I80 treatment. This is evidence that the spectral reflectance of African eggplant canopy in the visible and near infrared parts of the spectrum responds accordingly to N variation (Prudnikova et al., 2019). Additionally, Elvanidi et al. (2018) recommended the need for more research on the use of spectral based indices to detect N status, for improving tomato growth under deficit irrigation. Contradicting results across different types of crops confirm

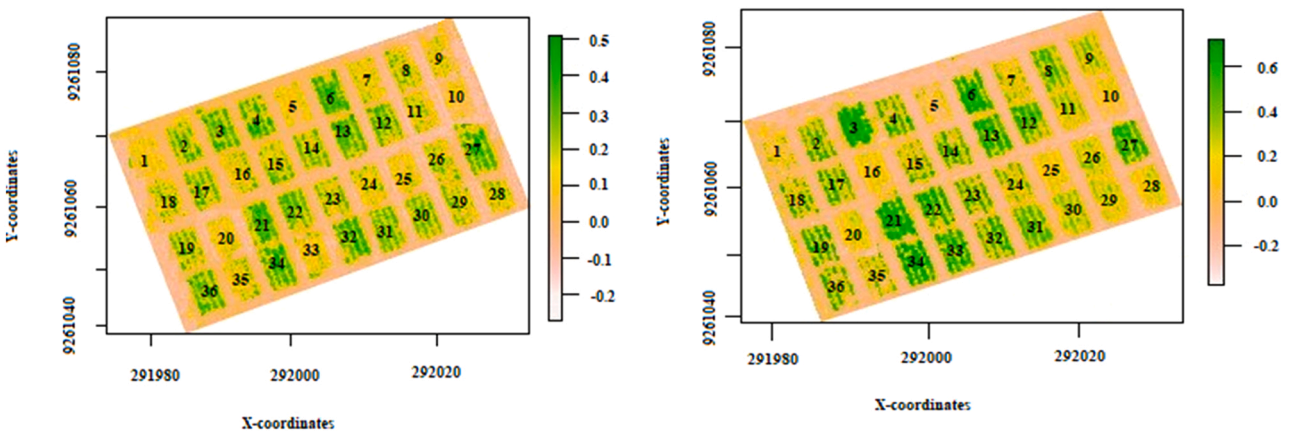

Fig. 8. Spatial maps using GNDVI (left) and NDVI (right) values indicating different interaction levels of water and nitrogen. Note: Plots 12, 13 and 34 represent I100F100; 6,8 and 33 represent I100F75; 11,14 and 22 represent I100F50; 5,7 and 21 represent I100F0; 3, 23 and 30 represent I80F100; 4,29 and 32 represent I80F75; 16,26 and 31 represent I80F50; 15, 24 and 25 represent I100F0; 9, 17 and 19 represent I60F100; 2,28,36 represent I60F75; 18,20 and 27 represent I60F50; 1,10 and 35 represent I60F0.

Table 6
Correlation (R^2) between fruit yield and vegetation indices.

Vegetation indices	Crop stage						
	Initial stage	Vegetative stage			Full vegetative stage		
	R^2	R^2	P-value	Equation	R^2	P-value	Equation
EVI2	NS	NS			NS		
GNDVI	NS	0.34	7.2×10^{-8}	$y = 0.21 + 0.0032x$	0.47	2.3×10^{-11}	$y = 0.096 + 0.0033x$
GRVI	NS	NS			NS		
NDVI	NS	0.46	4.7×10^{-11}	$y = 0.2 + 0.0062x$	0.53	5.9×10^{-13}	$y = 0.12 + 0.0087x$
OSAVI	NS	0.47	4.1×10^{-11}	$y = 0.24 + 0.004x$	0.52	2.8×10^{-9}	$y = 0.14 + 0.0062x$
SAVI	NS	NS			NS		
TDVI	NS	NS			NS		
NDRE	NS	NS			NS		

NS = Not significant at 0.05 significance level

that plants respond differently to incoming light spectra hence there is a need for plant specific calibrations.

4.2. The response of vegetation indices to detect the interactive effect of water and N and predict Eggplant yield

In general, the findings of this study indicated that water and nitrogen causes plant tissues in horticultural crops to reflect more in the NIR and green spectral bands. This has been reported for other crops such as wheat, lint and pinto bean (Ballester et al., 2019; Kyratzis et al., 2017; Ranjan et al., 2019). The interaction of water and N combination significantly affects the internal leaf structure causing a significant difference in the reflectance of the NIR band of the electromagnetic radiation. The reflectance within the green band was also significantly different in various treatments thus increasing the response of the GNDVI. The response of these bands in numerous water and N combinations, was thus capable to distinguish between healthy and unhealthy plants.

Among the vegetation indices tested, the GNDVI, NDVI and OSAVI were moderately sensitive to the interaction of water and N at vegetative and full vegetative stages. At the vegetative cropping stage, the GNDVI and NDVI performed slightly better compared to OSAVI in detecting differences in canopy reflectance. Across treatments GNDVI was able to detect both the high and low N application levels. The GNDVI therefore can be used to show areas with water and N stress within the field (Candiago et al., 2015). Furthermore, GNDVI performed better in detecting the response of African eggplant to different N levels under I100 whilst NDVI seemed to perform stronger in detecting differences of plant response to N levels under I80. The results are in agreement with Candiago et al. (2015) who found that GNDVI was capable in detecting changes in plant chlorophyll and those of Bhandari et al. (2018) for NDVI. OSAVI was also sensitive in distinguishing treatments with highest levels of inputs (water and N) from the rest. The index was sensitive to showing a decline in water and N as most treatments with 60% water have low values of indices as compared to those with 80% and 100% water.

Furthermore, GNDVI in the vegetative stage allowed for a clearer distinction between groups in function of the water and N treatment. GNDVI was able to classify 11 out of 12 treatments into 5 groups. Treatments in these groups resembled similarities in canopy reflectance. For example, whilst I100F100 was clearly differentiated from all other treatments, the reflectance between 75% application of N under I100 and I80 was found to be similar to 100% of N application under I80. Similarly, 50% of N application under I100 showed a similar average reflectance to 100% N application under I60. This further confirms the partial ability of plants to compensate for either water or nitrogen deficiency if one of these two inputs is available in higher amounts (Mwinuka et al., 2021a). The fact that a certain amount of irrigation water can optimize the efficiency of nutrients uptake by the plant is an important criterion to consider in agricultural water management (Xiang et al., 2019). At the full vegetative stage, GNDVI performed less well than NDVI as the latter was able to classify 7 treatments out of 12 into 5 groups. These groups resembled mainly the combinations of high water and nitrogen inputs and those with higher deficiencies in water or nitrogen.

The complexity of N and water interaction on plant performance resulted in GNDVI, NDVI and OSAVI showing a moderate potential to predict end of the season fruit yield. These results are similar to Sultana

et al. (2014) and Tuvdendorj et al. (2019) who found that the NDVI could predict wheat yield. Except for NDVI and OSAVI at full vegetative stages, correlation was below 50%. Results in this study showed a lower correlation compared to the earlier findings of Mwinuka et al. (2021b) for predicting African eggplant based on irrigation treatment alone.

The variability in capability of GNDVI, NDVI and OSAVI to detect differences in canopy performance and the moderate correlation suggest the need for a combined VI approach. Developing a decision tree using a combination of all three VI and both stages could support better treatment identification, as individual threshold detection is difficult given the interactive effect of water and nitrogen on plant development.

4.3. Vegetation indices maps

Vegetation indices maps were able to identify different water and nitrogen treatments during the vegetative and full vegetative stages of crop development. These findings are similar to Wang et al. (2016), Omer et al. (2017) among others. The differences in canopy reflectance are due to different plant chemical and physiological properties caused by the variation of water and N. Within the field, the healthier plants are identified by a higher value of VI (i.e. green color on the map) whilst unhealthy plants showed lower values (i.e. yellow color on the map). The VI was significantly higher ($p < 0.01$) when they were calculated using the NIR and red spectral bands such as NDVI and OSAVI. In agreement with these findings, Ge et al. (2019) found that the highest reflectance of NIR was observed in healthy plants due to multiple reflections of the turgid cell structure. This concludes that identification of spatial variation in water and N management for horticultural crops under tropical sub-humid conditions can be carried out using vegetation indices maps.

5. Conclusions

This study aimed to assess the ability of UAV-based multispectral vegetation indices in detecting the interactive effect of water and nitrogen management in irrigated horticultural crop production under tropical sub-humid climate. Vegetation indices showed a varying capability of distinguishing between crop responses following different water and N treatments and their combination. For instance, the TDVI performed best in detecting leaf moisture changes as a function of irrigation treatment irrespective of the N treatment at the vegetative stage. Nitrogen variation within the plant canopy was best distinguished by GNDVI during vegetative and full vegetative stages irrespective of irrigation treatment. The NDVI and OSAVI worked well to differentiate canopy N at full vegetative stage.

When it came to water and nitrogen interaction, GNDVI, NDVI and OSAVI potential in detecting significant differences between treatments varied. This is related to the spectral bands used, and ability to detect changes in the plant tissue as well as the plants ability to moderately compensate for water or nitrogen limitations. The study revealed that if one of the inputs are less limiting, the effect on canopy reduction is less pronounced, challenging the differentiation using a VI and therefore ability to predict season yields.

Generally, the study observed that vegetation indices are most effective when they are used to assess water and N separately. The interactive effect of water and N on African eggplant would require crop specific multi VI calibration given the advantages that all three VI showed for specific treatments. The fact that a certain amount of irrigation water can optimize the efficiency of nutrients uptake by the plant is an important criterion to consider in developing crop specific VI based decision trees for crop performance assessments and yield prediction.

Declaration of Competing Interest

The authors declare that they have no known competing financial interests or personal relationships that could have appeared to influence the work reported in this paper.

Acknowledgements

The authors would like to acknowledge the Feed the Future Innovation Laboratory for Small Scale Irrigation Programme through the U.S. Agency for International Development under the terms of Contract Number AID-OAA-A-13-0055. The opinions expressed herein are those of the authors and do not necessarily reflect the views of the U.S. Agency for International Development. The authors also do acknowledge the Sokoine University of Agriculture from Tanzania and the International Water Management Institute for their technical support. Likewise, authors give thanks to the Soil-Water Management Team from the Department of Engineering Sciences and Technology, under Prof. F.C. Kahimba (team leader), who facilitated us during the period of implementing the research. Moreover, the authors do acknowledge Mr. Justine Maisha and Ms. Mary Sauga for their support during data collection.

References

Badzmierowski, M.J., McCall, D.S., Evanylo, G., 2019. Using hyperspectral and multispectral indices to detect water stress for an urban turfgrass system. Agronomy 9 (8), 439. https://doi.org/10.3390/agronomy9080439.

Ballester, C., Brinkhoff, J., Quayle, W.C., Hornbuckle, J., 2019. Monitoring the Effects of Water Stress in CottonUsing the Green Red Vegetation Index and Red Edge Ratio. Remote Sens. 11 (7), 873. https://doi.org/10.3390/rs11070873.

Bellvert, J., Marsal, J., Girona, J., Zarco-Tejada, P.J., 2015. Seasonal evolution of crop water stress index ingrapevine varieties determined with high-resolution remote sensing thermalimagery. Irrig. Sci. 33 (2), 81–93. https://doi.org/10.1007/s00271-014-0456-y.

Benor, M., Levy, G.J., Mishael, Y., Nadler, A., 2013. Salinity effects on the fieldscout TDR 300 soil moisture meter readings. Soil Sci. Soc. Am. J. 77 (2), 412–416. https://doi.org/10.2136/sssaj2012.0294n.

Berni, J.A.J., Zarco-Tejada, P.J., Sepulcre-Cantó, G., Fereres, E., Villalobos, F., 2009. Mapping canopy conductance and CWSI in olive orchards using high resolution thermal remote sensing imagery. Remote Sens. Environ. 113 (11), 2380–2388. https://doi.org/10.1016/j.rse.2009.06.018.

Bhandari, S., Raheja, A., Chaichi, M., Green, R., Do, D., Pham, F., Ansari, M., Wolf J.G., Sherman, T.M. Espinas, A., 2018. Effectiveness of UAV-based remote sensing techniques in determining lettuce nitrogen and water stresses. In Proceedings of 14th International Conference on Precision Agriculture (pp. 1066403–1066415). https://doi.org/10.1109/icuas.2018.8453445.

Bronson, K.F., White, J.W., Conley, M.M., Hunsaker, D.J., Thorp, K.R., French, A.N., Holland, K.H., 2017. Active optical sensors in irrigated durum wheat: nitrogen and water effects. Agron. J. 109 (3), 1060–1071. https://doi.org/10.2134/agronj2016.07.0390.

Cabrera-Bosquet, L., Molero, G., Stellacci, A., Bort, J., Nogues, S., Araus, J., 2011. NDVI as a potential tool for predicting biomass, plant nitrogen content and growth in wheat genotypes subjected to different water and nitrogen conditions. Cereal Res. Commun. 39 (1), 147–159. https://doi.org/10.1556/crc.39.2011.1.15.

Cambui, C.A., Svennerstam, H., Gruffman, L., Nordin, A., Ganeteg, U., Näsholm, T., 2011. Patterns of plant biomass partitioning depend on nitrogen source. PLoS One 6 (4), e19211. https://doi.org/10.1371/journal.pone.0019211.

Candiago, S., Remondino, F., De Giglio, M., Dubbini, M., Gattelli, M., 2015. Evaluating multispectral images and vegetation indices for precision farming applications from UAV images. Remote Sens. 7 (4), 4026–4047. https://doi.org/10.3390/rs70404026.

Chen, J.B., Dong, C.C., Yao, X.D., Wang, W., 2018. Effects of nitrogen addition on plant biomass and tissue elemental content in different degradation stages of temperate steppe in northern China. J. Plant Ecol. 11 (5), 730–739. https://doi.org/10.1093/jpe/rtx035.

Çolak, Y.B., Yazar, A., Çolak, İ., Akça, H., Duraktekin, G., 2015. Evaluation of crop water stress index (CWSI) for eggplant under varying irrigation regimes using surface and subsurface drip systems. Agric. Agric. Sci. Procedia 4, 372–382. https://doi.org/10.1016/j.aaspro.2015.03.042.

Corti, M., Gallina, P.M., Cavalli, D., Cabassi, G., 2017. Hyperspectral imaging of spinach canopy undercombined water and nitrogen stress to estimate biomass, water, and nitrogencontent. Biosyst. Eng. 158, 38–50. https://doi.org/10.1016/j.biosystemseng.2017.03.006.

El Nahry, A.H., Ali, R.R., El Baroudy, A.A., 2011. An approach for precision farming under pivot irrigation system using remote sensing and GIS techniques. Agric. Water Manag. 98 (4), 517–531. https://doi.org/10.1016/j.agwat.2010.09.012.

Elvanidi, A., Katsoulas, N., Kittas, C., 2018. Automation for water and nitrogen deficit stress detection in soilless tomato crops based on spectral indices. Horticulturae 4 (4), 47. https://doi.org/10.3390/horticulturae4040047.

Fang, M., Ju, W., Zhan, W., Cheng, T., Qiu, F., Wang, J., 2017. A new spectral similarity water index for the estimation of leaf water content from hyperspectral data of leaves. Remote Sens. Environ. 196, 13–27. https://doi.org/10.1016/j.rse.2017.04.029.

Fondio, L., N'Gbesso, M.F.D.P., Coulibaly, N.D., 2016. Effect of mineral fertilization on African eggplant (Solanum spp.) Productivity in Côte d'Ivoire. J. Agric. Sci. Technol. https://doi.org/10.17265/2161-6264/2016.03.006.

Ge, Y., Atefi, A., Zhang, H., Miao, C., Ramamurthy, R.K., Sigmon, B., Yang, J., Schnable, J.C., 2019. High-throughput analysis of leaf physiological and chemical traits with VIS–NIR–SWIR spectroscopy: a case study with a maize diversity panel. Plant Methods 15 (1), 66. https://doi.org/10.1186/s13007-019-0450-8.

Ge, Y., Bai, G., Stoerger, V., Schnable, J.C., 2016. Temporal dynamics of maize plantgrowth, wateruse, and leaf water content using automated high throughput RGBandhyperspectral imaging. Comput. Electron. Agric. 127, 625–632. https://doi.org/10.1016/j.compag.2016.07.028.

Irfan, M., Ahmed, Z.I., Khan, T.A., Ahmad, W., Akhtar, M.T., Iqbal, K., Malik, M.N., 2018. Monitoring of wheat and rice nitrogen status by remote sensing. J. Exp. Agric. Int. 1–13. https://doi.org/10.9734/JEAI/2018/16566.

Julitta, T., Corp, L.A., Rossini, M., Burkart, A., Cogliati, S., Davies, N., Hom, M., Mac Arthur, A., Middleton, E.M., Rascher, U., Schickling, A., Colombo, R., 2016. Comparison of sun-induced chlorophyll fluorescence estimates obtained from four portable field spectroradiometers. Remote Sens. 8 (2) https://doi.org/10.3390/rs8020122.

Kadiyala, D. M., 2012. Optimizing Cultural Practicesfor Saving Water and Nitrogen for Rice-Maize Cropping System in Semi-AridTropics (Doctoral dissertation, University of Florida).

Klem, K., Záhora, J., Zemek, F., Trunda, P., Tůma, I., Novotná, K., Hodaňová, P., Rapantová, B., Hanuš, J., Vavříková, J., Holub, P., 2018. Interactive effects of water deficit and nitrogen nutrition on winter wheat. Remote sensing methods for their detection. Agric. Water Manag. 210, 171–184. https://doi.org/10.1016/j.agwat.2018.08.004.

Kyratzis, A.C., Skarlatos, D.P., Menexes, G.C., Vamvakousis, V.F., Katsiotis, A., 2017. Assessment of vegetation indices derived by UAV imagery for durum wheat phenotyping under a water limited and heat stressed mediterranean environment. Front. Plant Sci. 8, 1114. https://doi.org/10.3389/fpls.2017.01114.

Liu, C.W., Sung, Y., Chen, B.C., Lai, H.Y., 2014. Effects of nitrogen fertilizers on the growth and nitrate content of lettuce (Lactuca sativa L.). Int. J. Environ. Res. Public Health 11 (4), 4427–4440. https://doi.org/10.3390/ijerph110404427.

Mee, C., Siva, K.B., Ahmad, H.M.H., 2017. Detecting and monitoring plant nutrient stress using remote sensing approaches: a review. Asian J. Plant Sci. 16 (1), 1–8. https://doi.org/10.3923/ajps.2017.1.8.

Moncada, A., Vetrano, F., Esposito, A., Miceli, A., 2020. Fertigation management and growth-promoting treatments affect tomato transplant production and plant growth after transplant. Agronomy 10 (10), 1504. https://doi.org/10.3390/agronomy10101504.

Mulla, D.J., 2013. Twenty-five years of remote sensing in precision agriculture: key advances and remaining knowledge gaps. Biosyst. Eng. 114 (4), 358–371. https://doi.org/10.1016/j.biosystemseng.2012.08.009.

Mwinuka, P.R., Mbilinyi, B.P., Mbungu, W.B., Mourice, S.K., Mahoo, H.F., Schmitter, P., 2021a. Optimizing water and nitrogen application for neglected horticultural species in tropical sub-humid climate areas: a case of African eggplant (Solanum aethiopicum L.). Sci. Hortic. 276, 109756 https://doi.org/10.1016/j.scienta.2020.109756.

Mwinuka, P.R., Mbilinyi, B.P., Mbungu, W.B., Mourice, S.K., Mahoo, H.F., Schmitter, P., 2021b. The feasibility of hand-held thermal and UAV-based multispectral imaging for canopy water status assessment and yield prediction of irrigated African eggplant (Solanum aethopicum L). Agric. Water Manag., 106584 https://doi.org/10.1016/j.agwat.2020.106584.

Omer, G., Mutanga, O., Abdel-Rahman, E.M., Peerbhay, K., Adam, E., 2017. Mapping leaf nitrogen and carbon concentrations of intact and fragmented indigenous forest ecosystems using empirical modeling techniques and WorldView-2 data. ISPRS J. Photogramm. Remote Sens. 131, 26–39. https://doi.org/10.1016/j.isprsjprs.2017.07.005.

Park, S., Nolan, A., Ryu, D., Fuentes, S., Hernandez, E., Chung, H., O'connell, M., 2015. Estimation of crop water stress in a nectarine orchard using high-resolution imagery from unmanned aerial vehicle (UAV). In Proceedings of the 21st International Congress on Modelling and Simulation, Gold Coast, Australia (Vol. 29). https://doi.org/10.3390/rs9080828.

Petrie, P.R., Wang, Y., Liu, S., Lam, S., Whitty, M.A., Skewes, M.A., 2019. The accuracy and utility of a low cost thermal camera and smartphone-based system to assess grapevine water status. Biosyst. Eng. 179, 126–139. https://doi.org/10.1016/j.biosystemseng.2019.01.002.

Picoli, M.C.A., Duft, D.G., Machado, P.G., 2017. Identifying drought events in sugarcane using drought indices derived from Modis sensor. Pesqui. Agropecuária Bras. 52 (11), 1063–1071. https://doi.org/10.1590/s0100-204x2017001100012.

Patwardhan, A.S., Nieber, J.L., Johns, E.L., 1990. Effective rainfall estimation methods. J. Irrig. Drain. Eng. 116 (2), 182–193. https://doi.org/10.1061/(asce)0733-9437(1990)116:2(182).

Poblete-Echeverría, C., Espinace, D., Sepúlveda-Reyes, D., Zúñiga, M., Sanchez, M., 2017. Analysis of crop water stress index (CWSI) for estimating stem water potential in grapevines: comparison between natural reference and baseline approaches. Acta Hortic. 1150, 189–194. https://doi.org/10.17660/actahortic.2017.1150.27.

Prudnikova, E., Savin, I., Vindeker, G., Grubina, P., Shishkonakova, E., Sharychev, D., 2019. Influence of soil background on spectral reflectance of winter wheat crop canopy. Remote Sens. 11 (16), 1932. https://doi.org/10.3390/rs11161932.

Qin, W., 2015. Exploring options for improving water and nitrogen use efficiency in crop production systems (Doctoral dissertation, Wageningen University). ⟨https://wur.on.worldcat.org/v2/search?queryString=Exploring+options+for+improving+water+and+nitrogen+use+efficiency+in+crop+production+systems⟩+. ((Accessed on 11th August 2021).

Ranjan, R., Chandel, A.K., Khot, L.R., Bahlol, H.Y., Boydston, J., Miklas, R.A., Miklas, P. N., 2019. Irrigated pinto bean crop stress and yieldassessment using ground based lowaltitude remote sensing technology. Inf. Process. Agric. 6 (4), 502–514. https://doi.org/10.1016/j.inpa.2019.01.005.

Reyes-Gonzalez, A., 2017. Using Remote Sensing to Estimate Crop Water Use to Improve Irrigation Water Management. ⟨https://openprairie.sdstate.edu/etd/1708/⟩. (Accessed on 15 July 2020).

Restuccia, R., 2021. Quick Guide: Soil Moisture Sensors. ⟨https://jainsusa.com/blog/quick-guide-soil-moisture-sensors/⟩. (Accessed 9 August 2021).

RSA, 2012. Production guidelines for Tomato. https,//doi.org/10.3389/fphys.2012.00155 (Accessed 7 August 2017).

Team, R., 2018. RStudio: Integrated Development for R. RStudio, Inc., Boston, MA ⟨http://www.rstudio.com/⟩.(Accessed on 15 July 2021).

Shiratsuchi, L., Ferguson, R., Shanahan, J., Adamchuk, V., Rundquist, D., Marx, D., Slater, G., 2011. Water and nitrogen effects on active canopy sensor vegetation indices. Agron. J. 103 (6), 1815–1826. https://doi.org/10.2134/agronj2011.0199.

Stone, K.C., Bauer, P.J., Sigua, G.C., 2016. Irrigation management using an expert system, soil water potentials, and vegetative indices for spatial applications. Trans. ASABE 59 (3), 941–948. https://doi.org/10.13031/trans.59.11550.

Sultana, S.R., Ali, A., Ahmad, A., Mubeen, M., Zia-Ul-Haq, M., Ahmad, S., Ercisli, S., Jaafar, H.Z., 2014. Normalized difference vegetation index as a tool for wheat yield estimation: a case study from Faisalabad, Pakistan. Sci. World J. 2014. https://doi.org/10.1155/2014/725326.

Tripathi, R., Nayak, A.K., Raja, R., Shahid, M., Mohanty, S., Lal, B., Gautam, P., Panda, B. B., Kumar, A., Sahoo, R.N., 2017. Site-specific nitrogen management in rice using remote sensing and geostatistics. Commun. Soil Sci. Plant Anal. 48 (10), 1154–1166. https://doi.org/10.1080/00103624.2017.1341907.

Tuvdendorj, B., Wu, B., Zeng, H., Batdelger, G., Nanzad, L., 2019. Determination of appropriate remote sensing indices for spring wheat yield estimation in mongolia. Remote Sens. 11 (21), 2568. https://doi.org/10.3390/rs11212568.

Ustuner, M., Sanli, F.B., Abdikan, S., Esetlili, M.T., Kurucu, Y., 2014. Crop type classification using vegetation indices of rapideye imagery. The International Archives of Photogrammetry. Remote Sens. Spat. Inf. Sci. 40 (7), 195. https://doi.org/10.5194/isprsarchives-xl-7-195-2014.

Wang, Z., Wang, T., Darvishzadeh, R., Skidmore, A.K., Jones, S., Suarez, L., Woodgate, W., Heiden, U., Heurich, M., Hearne, J., 2016. Vegetation indices for mapping canopy foliar nitrogen in a mixed temperate forest. Remote Sens. 8 (6), 491. https://doi.org/10.3390/rs8060491.

Xiang, Y., Zou, H., Zhang, F., Qiang, S., Wu, Y., Yan, S., Wang, H., Wu, L., Fan, J., Wang, X., 2019. Effect of irrigation level and irrigation frequency on the growth of mini Chinese cabbage and residual soil nitrate nitrogen. Sustainability 11 (1), 111. https://doi.org/10.3390/su11010111.

Xue, J., Su, B., 2017. Significant remote sensing vegetation indices: a review of developments and applications. J. Sens. 2017. https://doi.org/10.1155/2017/1353691.

Yuan, S., Peng, S., 2017. Exploring the trends in nitrogen input and nitrogen use efficiency for agricultural sustainability. Sustainability 9 (10), 1905. https://doi.org/10.3390/su9101905.

Zhang, Y., Han, W., Niu, X., Li, G., 2019. Maize crop coefficient estimated from UAV-measured multispectral vegetation indices. Sensors 19 (23), 5250. https://doi.org/10.3390/s19235250.

Zou, X., Mõttus, M., 2017. Sensitivity of common vegetation indices to the canopy structure of field crops. Remote Sens. 9 (10), 994. https://doi.org/10.3390/rs9100994.

Zotarelli, L., Scholberg, J.M., Dukes, M.D., 2009. Tomato yield, biomass accumulation, root distribution and irrigation water use efficiency on a sandy soil, as affected by nitrogen rate and irrigation scheduling. Agric. Water Manag. 96, 23–34. https://doi.org/10.1016/j.agwat.2008.06.007.